

Smartphone MEMS Accelerometer for Cycling – Observations

Sara Stančin, Sašo Tomažič

University of Ljubljana, Faculty of electrical engineering, Ljubljana, Slovenia
sara.stancin@fe.uni-lj.si, saso.tomazic@fe.uni-lj.si

Abstract— Equipped with 3D MEMS sensors, today's smartphones provide for a wide range of practical measurements. However, MEMS sensors are characterized by different errors including zero level offset, inaccurate sensitivity, axis misalignment and noise. Bearing these inaccuracies in mind, we investigate the feasibility of using a smartphone 3D accelerometer during cycling and provide with some practical observations. Using the accelerometer, we track the slope of the road. Binding the obtained road slope profile with the GPS speed measurements, we estimate motion altitude change. We conclude that, if suitably calibrated, the accelerometer can be feasible for this purpose. However, even small errors in gravity projections estimates lead to significant errors in altitude change estimation. Due to integration, measurement noise contributes less to the estimated altitude error.

I. INTRODUCTION

A 3D accelerometer enables measurements of acceleration caused by gravity and self-accelerated motion along the three orthogonal sensitivity axes. As such, accelerometers are increasingly being used for simple and frequent human motion measurements enabling human motion capture [1, 2], monitoring [3, 4], analysis and characterization [5-10]. Different support for rehabilitation [11-13] as well as for augmented and virtual reality [14, 15] has been proposed.

Today available kinematic sensors that are based on Microelectromechanical systems (MEMS) are small, light, widely affordable, and come with their own battery supply. These sensors cause minimal physical obstacles for motion performance and can provide simple, repeatable, and collectible motion data indoors. Moreover, because of their low energy consumption, MEMS sensors are a promising tool for tracking motion outdoors.

Widely available low-cost MEMS sensors are characterized by different types of sensor inaccuracies (including the zero level offset, inaccurate sensitivity and misalignment of the sensor sensitivity axes), temperature drift and noise. If non-negligible acceleration is present in the motion, the typical obstacle is the correct deduction of the gravitational acceleration from the total measured acceleration. Because the position data are obtained by integrating the acceleration twice, even small errors in the determined direction of acceleration can cause the calculated position to deviate considerably from the true sensor position. Due to the accumulation of position error, efficient implementation of navigation applications using low cost MEMS accelerometers and gyroscopes alone is not possible.

In this research, we investigate the feasibility of using a smartphone 3D accelerometer during cycling. We focus on the road slope and altitude change estimation.

By providing for load monitoring and energy management, these data are very valuable to the average recreational or professional cyclist.

The result of the accelerometer sensitivity to gravity is that when at rest, the accelerometer shows 1 g of acceleration along the axis of sensitivity oriented along the direction normal to the horizontal surface. This makes it easy to determine the orientation with respect to the direction of the vector of gravitational acceleration in the accelerometer coordinate system.

It is a necessary condition that the accelerometer is either stationary either moving with negligible acceleration in relation to the gravitational acceleration either that the speed of the accelerometer is also by some mean known.

For our purpose, we focus on the first scenario and track bicycle motion characterized by negligible acceleration in relation to the gravitational acceleration. In such a way, the projections of gravity onto the sensor sensitivity axes directly reflect the slope of the road.

Further on, by binding the accelerometer measurements with speed data, we estimate motion altitude change.

II. BICYCLE MEASUREMENT SETUP

To investigate the feasibility of a smartphone accelerometer for tracking road slope and altitude change during cycling, we mounted an iPhone 4S on the handlebar of a bicycle as shown in Figure 1.

The orientation of the smartphone accelerometer intrinsic coordinate system is as illustrated in Figure 1. φ_0 refers to the angle between the sensor and the direction of motion. In further text, we will refer to this angle as the accelerometer level angle.

The smartphone accelerometer is designed in such a way that when at rest it measures 1g of acceleration along the downwards pointed axis.

In this experiment, we relied on the GPS system for the speed measurements. The GPS receiver position data errors are in 10 m range. Speed obtained by tracking position change is for this reason highly unreliable. However, the GPS also provides for speed measurements based on the Doppler effect. For our purpose, these have shown to be much more reliable.

To capture both, the accelerometer and GPS data at common times samples, we used the iPhone SensorLog application. The measurement range of the accelerometer is set to $\pm 2g$ and cannot be changed.

An alternative for obtaining the reference speed is using a dedicated bicycle speed measurement unit. Such a unit tracks wheel rpm and in such a way provides for onsite speed measurements. In such a measurement setup, the user would have to provide for efficient synchronization of the accelerometer and the speed measurement unit.

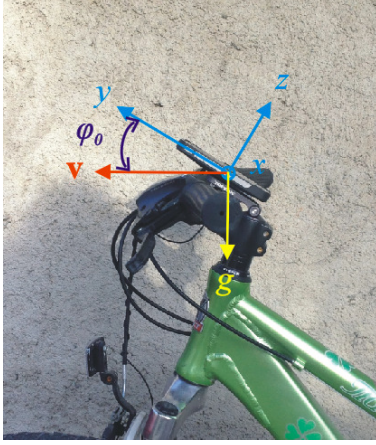


Figure 1. Side view of the smartphone position on the handlebar of the bicycle.

III. ACCELEROMETER CALIBRATION

When analyzing motion dynamics, just as in the case of absolute motion values estimation, accurate data are the basis for an effective and a comprehensive analysis. The accuracy of the captured data is essential for relevant and comparable results. The first step in motion data capture and analysis is hence sensor calibration.

According to the generally adapted model, the accuracy of the values measured with a 3D sensor is influenced by the accuracy of the sensor axis sensitivity, zero level offset and orientation.

The aim of different calibration procedures is to compensate for the measurement errors that arise because of the enlisted inaccuracies.

Considering static calibration, we need to obtain values of 12 calibration parameters. 3 of these are needed to compensate for zero level offset and the remaining nine compensate for axes misalignment and inaccurate sensitivity.

Different procedures have been proposed in order to achieve sensor calibration. We performed the 3D accelerometer calibration according to the procedure we have already presented in [16]. This procedure provides for, in terms of lifetime and computational complexity, an efficient calibration procedure that does not require any additional expensive equipment and is suitable for everyday practical use.

The procedures exploit the fact that the value of the measured acceleration at rest is constant and equal to gravity acceleration. To estimate the values of the 12 calibration parameters contained, six measurements are needed. During these six measurements, the sensor is at rest on an even horizontal surface in turn in six different orientations. The orientations of the first three measurements are such that the sensor intrinsic axes x , y , and z show in turn in the direction of the gravity vector \mathbf{g} . The orientations of remaining three measurements are

such that the sensor intrinsic axes x , y , and z show in turn in the opposite direction of the gravity vector \mathbf{g} .

For each of the six measurements, we obtained 10,000 samples. The obtained data are shown in Figures 2 and 3.

From these figures we can observe that each of the three sensor intrinsic sensitivity axis (x , y and z) has a negative zero level offset which is the greatest for the z -axis. The measurements are not symmetrical for pairs of measurements ($x/-x$, $y/-y$ and $z/-z$) from what we can conclude that the axis are not perfectly aligned.

Averaging values detected for each of the six measurements, matrices \mathbf{A}_{s+} and \mathbf{A}_{s-} were calculated. The columns of both of these matrices are equal to the vectors of the detected acceleration values for each of the three measurements, and the rows represent the sensitivity axes. Matrix \mathbf{A}_{s+} combines the three measurements when the three sensor coordinate axes x , y and z is, in turn, aligned with the direction of \mathbf{g} . Matrix \mathbf{A}_{s-} combines the three measurements when the three sensor coordinate axes are in turn, aligned with the direction opposite to the direction of \mathbf{g} .

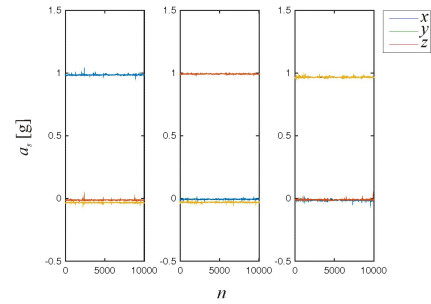


Figure 2. iPhone 4s 3D accelerometer collected data for the first three calibration measurements. During these measurements, the sensor orientations were set such that the sensor's intrinsic coordinate axes (x , y and z) were aligned in turn along the direction of the gravity vector \mathbf{g} .

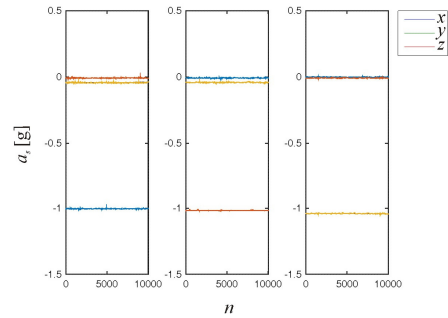


Figure 3. iPhone 4s 3D accelerometer collected data for the remaining three calibration measurements. During these three measurements, the sensor orientations were set such that the sensor's intrinsic coordinate axes (x , y and z) were aligned in turn opposite to the direction of the gravity vector \mathbf{g} .

Using matrices \mathbf{A}_{s+} and \mathbf{A}_{s-} we obtain the zero level offset vector and the calibration matrix according to [16]:

$$\mathbf{a}_o = \frac{(\mathbf{A}_{s+} + \mathbf{A}_{s-}) \times \mathbf{i}}{6} \quad (1)$$

$$\mathbf{C}_s = 2(\mathbf{A}_{s+} - \mathbf{A}_{s-})^{-1} \quad (2)$$

Values obtained for the used iPhone 4S device were:

$$\mathbf{a}_o = \begin{bmatrix} -0.0066 \\ -0.0094 \\ -0.0358 \end{bmatrix} \quad (3)$$

$$\mathbf{C}_s = \begin{bmatrix} 1.0058 & -0.0004 & 0.0067 \\ 0.0029 & 0.9958 & 0.0013 \\ -0.0050 & -0.0050 & 0.9969 \end{bmatrix} \quad (4)$$

Each acceleration measurement triplet \mathbf{a}_s is then corrected according to:

$$\mathbf{a} = \mathbf{C}_s \times (\mathbf{a}_s - \mathbf{a}_o) \quad (5)$$

From the zero level offset results (3), we can conclude that, as expected, the zero level offset is the greatest for the z -axis.

From the obtained calibration matrix (4), we can estimate the vector of accelerometer sensitivities \mathbf{S} :

$$\mathbf{S} = \begin{bmatrix} 0.9942 \\ 1.0042 \\ 1.0031 \end{bmatrix} \quad (6)$$

where each vector element represents the sensitivity of the respective axis for the used accelerometer.

From the obtained calibration matrix (4), we can also estimate the sensitivity axes alignment matrix:

$$\mathbf{\Psi} = \begin{bmatrix} 0.3857 & 89.9789 & 90.3851 \\ 90.1656 & 0.1812 & 90.0736 \\ 89.7160 & 89.7122 & 0.4043 \end{bmatrix}. \quad (7)$$

In the above matrix, all angles are given in degrees. The rows of matrix $\mathbf{\Psi}$ represent the sensor sensitivity axes, and its columns represent the sensor coordinate axes. From (7) we can conclude that among the three axes of the used sensor, y -axis has the least misalignment.

IV. MEASUREMENT ANALYSIS

A Measurement route

The observed cycling route included a hill climb on an asphalt road with a total altitude change of 506 m. The whole route lasted 1 h.

B Measurement Data

The obtained measurement data was sampled in uneven sampling intervals ranging from 6 ms to 1.617 s. For this reason, both accelerometer and GPS measurements were interpolated to the shortest sampling interval from the original data. In such a way, we obtained data sampled at $f_s = 1/6\text{ms} = 166.7$ Hz.

Data obtained for all three sensor axes are illustrated in Figure 4.

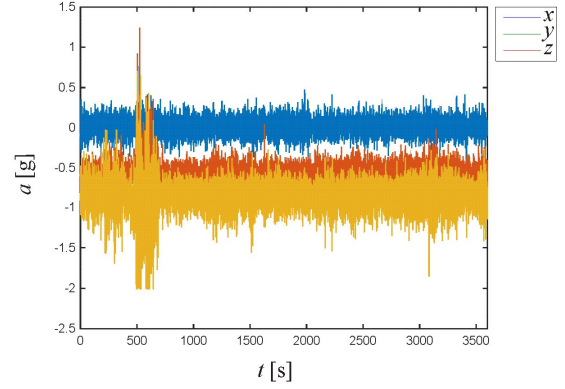


Figure 4. Measurement 3D acceleration data after calibration.

In further analysis, we made the following assumptions:

1. We supposed that the bicycle acceleration is neglectable in comparison to gravity. When cycling uphill, this is a reasonable assumption. This enables us to obtain the slope of the road considering the projection of gravity onto axes y and z . However, from Figure 4, we can observe high oscillations of the measured acceleration along all three axes that are a consequence of the roughness of the asphalt road. Due to the limited measurement range, these oscillations cause clipping of the measured data along the z -axis. For this reason, we could not rely on the z -axis acceleration data.
2. For our investigation, we simplified the problem and supposed that the lateral tilt of the bicycle is not affecting the gravity projection onto y -axis.

Under these assumptions, we can estimate the road slope considering only the acceleration measured along the y -axis. Considering the orientation of the sensor axes as illustrated in Figure 1, we can write:

$$\varphi = \cos^{-1} a_y - 90^\circ - \varphi_0 \quad (8)$$

where φ_0 is the accelerometer level angle (i.e., the angle between the accelerometer y -axis and the direction of motion - see Figure 1). This angle can be roughly estimated prior to measurements, from the a_y measurements at an approximately level surface.

Before actual road slope calculation, we filtered the re-sampled calibrated accelerometer outputs with a low pass filter. The cutoff frequency was chosen to be $f_{co} = 0.14$ Hz. As estimated, choosing this frequency provided for the best distinction between vibrations due to the roughness of the asphalt road and the true slope of the road.

C Results

Using the road slope and equally re-sampled GPS speed data, we can calculate the change in the bicycle altitude:

$$\Delta h = \sin(\varphi) v \Delta t \quad (9)$$

where v represents bicycle speed obtained from the GPS, Δt is the time interval and φ represents the road slope determined according to (6). The actual angle φ_0 in (6) is estimated by finding the best fit solution for height change determined according to (7) and GPS altitude data. The

best fit was obtained for $\varphi_0=31^\circ$. The resulting road slope φ throughout the experiment route is shown in Figure 6.

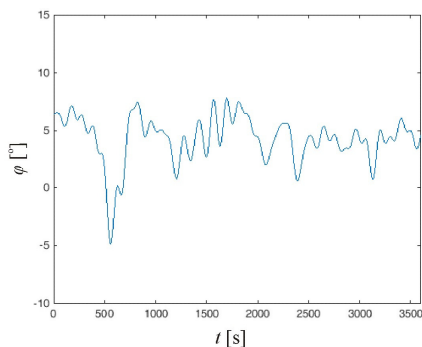


Figure 5. Road slope obtained from the smartphone accelerometer.

For result evaluation, we sum the altitude changes obtained according to (7) and compare them to GPS obtained altitude data. Altitude results for $\varphi_0=31^\circ$ are shown in Figure 6. GPS altitude data is shown as reference data. We can observe that the results match closely throughout the 1 h ride. The figure also shows the resulting altitude data obtained considering a small deviation in the level angle of the smartphone $\varphi_0=31.02^\circ$. At the beginning of the route, the accelerometer altitude data follows the GPS altitude. However, after a 1 h ride, an error of 0.02° in the estimated level angle causes a 30.84 m altitude estimate error.

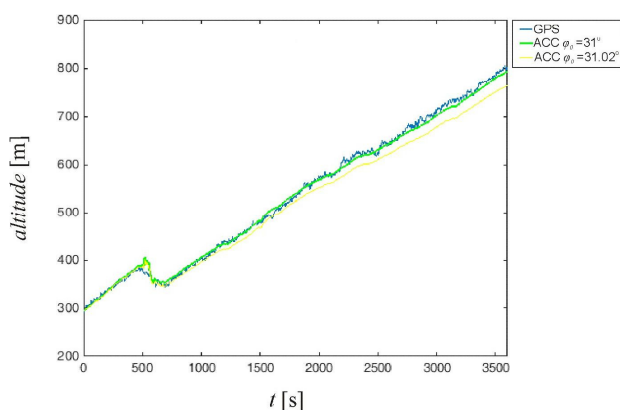


Figure 6. Altitude obtained from the smartphone accelerometer road slope data combined with GPS speed data.

V. CONCLUSION

From the results obtained, we can conclude that, if suitably calibrated, the smartphone accelerometer can be used for road slope tracking and altitude change estimate. In this article we presented a way of performing this task when the motion of the bicycle is characterized by negligible acceleration in relation to the gravitational acceleration. In such a way, the projections of gravity onto the sensor sensitivity axes directly reflect the slope of the road. Considering altitude change estimates, we can conclude that due to integration, even small errors in the estimated gravity projection cause immense errors in altitude estimation. Further on, integrating measurement noise has a low pass filtering effect and for this reason

noise itself contributed less to the error in the estimated altitude.

To achieve road slope and altitude estimation in general, highly accurate bicycle velocity data would be needed.

REFERENCES

- [1] Aminian, K., Najafi, B., Capturing human motion using body-fixed sensors: outdoor measurement and clinical application, *Comp. Anim. Virtual Worlds*, 15, pp. 79–94, 2004.
- [2] Roetenberg, D., Slycke, P.J., Veltink, P.H., Ambulatory Position and Orientation Tracking Fusing Magnetic and Inertial Sensing, *IEEE Trans. Biomed. Eng.*, 54(5), pp. 883–890, 2007.
- [3] Aminian, K., Robert, P., Buchser, E.E., Rutschmann, B., Hayoz, D., Depairon, M., Physical activity monitoring based on accelerometry: validation and comparison with video observation, *Med. Biol. Eng. Comput.*, 37, pp. 304–308, 1999.
- [4] Uiterwaal, M., Glerum, E.B.C., Busser, H.J., Lummel, R.C., Ambulatory monitoring of physical activity in working situations, a validation study, *J. Med. Eng. Tech.*, 22(4), pp. 168–172, 1998.
- [5] McIlwraith, D., Pansiot, J., Yang, G.Z., Wearable and ambient sensor fusion for the characterisation of human motion, 2010 IEEE/RSJ International Conference on Intelligent Robots and Systems (IROS), pp. 5505–5510, 2010.
- [6] Heinz, E.A., Kunze, K.S., Gruber, M., Bannach, D., Lukowicz, P., Using Wearable Sensors for Real-Time Recognition Tasks in Games of Martial Arts - An Initial Experiment, 2006 IEEE Symposium on Computational Intelligence and Games, pp. 98–102, 2006.
- [7] Hoffman, M., Varcholik, P., LaViola, J.J., Breaking the status quo: Improving 3D Gesture Recognition with Spatially Convenient Input Devices, *Proceedings of the 2010 IEEE Virtual Reality Conference (VR)*; Waltham, MA, USA. 20–24 March 2010, pp. 59–66, 2010.
- [8] Lin, P.C., Komsuoglu, H., Koditschek, D.E., Sensor data fusion for body state estimation in a hexapod robot with dynamical gaits, *IEEE Trans. Robot.*, 22, pp. 932–943, 2006.
- [9] Trifunovic, M., Vadiraj, A.M., Van Driel, W.D., MEMS accelerometers and their bio-applications, 13th International Conference on Thermal, Mechanical and Multi-Physics Simulation and Experiments in Microelectronics and Microsystems (EuroSimE), 16–18 Apr. 2012, pp. 1–7, 2012.
- [10] Stančin, S., Tomažič, S., Early Improper Motion Detection in Golf Swings Using Wearable Motion Sensors: The First Approach, *Sensors*, 12(6), pp. 7505–7521, 2013.
- [11] Brutovsky, N., Novak, D., Low-cost motivated rehabilitation system for post-operation exercises, *Engineering in Medicine and Biology Society*, 2006. EMBS '06. 28th Annual International Conference of the IEEE, pp. 6663–6666, 2006.
- [12] Zheng, H., Black, N.D., Harris, N.D., Position-sensing technologies for movement analysis in stroke rehabilitation, *J. Med. Biol. Eng. Comp.*, 43(4), pp. 413–420, 2005.
- [13] Liebermann, D.G., Berman, S., Weiss, P.L., Levin, M.F., Kinematics of Reaching Movements in a 2-D Virtual Environment in Adults With and Without Stroke, *IEEE Trans. Neural. Syst. Rehabil. Eng.*, 20(6), pp. 778–787, 2012.
- [14] Schall, G., Wagner, D., Reitmayr, G., Taichmann, E., Wieser, M., Schmalstieg, D., Hofmann-Wellenhof, B., Global Pose Estimation Using Multi-Sensor Fusion for Outdoor Augmented Reality. *Proceedings of the 8th IEEE International Symposium on Mixed and Augmented Reality ISMAR 2009*; Orlando, FL, USA. 19–22 October 2009, pp. 153–162, 2009.
- [15] Su, C., Xu, W., Mengnan, G., Shengquan, Y., Simulation Teaching in 3D Augmented Reality Environment, 2012 IIAI International Conference on Advanced Applied Informatics (IIAIAI), pp. 83–88, 2012.
- [16] Stančin, S., Tomažič, S., Time- and Computation-Efficient Calibration of MEMS 3D Accelerometers and Gyroscopes, *Sensors*, 14(8), pp. 14885–14915, 2014.